Applied and Computational Mechanics 4 (2010) 237–250

# Reconstruction of a fracture process zone during tensile failure of quasi-brittle materials

V. Veselý[a,*], P. Frantík[a]

[a] *Faculty of Civil Engineering, BUT Brno, Veveří 331/95, 602 00 Brno, Czech Republic*

Received 1 September 2009; received in revised form 4 October 2010

**Abstract**

The paper outlines a technique for estimation of the size and shape of an inelastic zone evolving around a crack tip during the tensile failure of structures/structural members made of quasi-brittle building materials, particularly cementitious composites. The technique is based on an amalgamation of several concepts dealing with the failure of structural materials, i.e. multi-parameter linear elastic fracture mechanics, classical non-linear fracture models for concrete (equivalent elastic crack and cohesive crack models), and the plasticity approach. The benefit of this technique is expected to be seen in the field of the determination of fracture characteristics describing the tensile failure of quasi-brittle silicate-based composites. The method is demonstrated using an example of a (numerically simulated) fracture test involving the three-point bending of a notched beam and validated by experimentally obtained results of three-point bending and wedge-splitting tests taken from the literature.


*Keywords:* cementitious composites, fracture, quasi-brittle, fracture process zone, multi-parameter linear elastic fracture mechanics, effective crack model, cohesive crack model, Rankine strength criterion

## 1. Introduction

Fracture of quasi-brittle materials is accompanied by formation and evolution of an inelastic zone around the propagating crack tip. This zone, referred to as the fracture process zone (FPZ), is responsible for the non-linear manner of the quasi-brittle fracture. In this zone the material is damaged via various failure mechanisms on several levels of material structure. The FPZ size can not be neglected in relation to the size of the structures/structural members made of quasi-brittle materials; it may be comparable in size to the material's basic constituents (e.g. the aggregate size in the case of cementitious composites) or be greater in extent by up to two orders of magnitude [5, 11, 21, 24]. The existence of this zone influences the values of fracture-mechanical properties determined by some of the standardized evaluation procedures from records of fracture tests, e.g. those based on the work-of-fracture method [18], as was extensively reported in literature (for the most relevant see [2, 7, 9, 12, 23]). This is caused by the fact, according to the opinion of the authors, see e.g. [29, 19], that the characteristics of the FPZ do not enter these evaluating procedures.

For determination of either the propagating crack tip position or rather the entire FPZ extension during the fracture process several experimental techniques have been reported in the literature (summarized e.g. in [21, 24]). Holographic interferometry technique was used in combination with digital image analysis to determine the FPZ extent from specimen surface

*Corresponding author. Tel.: +420 541 147 362, e-mail: vesely.v1@fce.vutbr.cz.

strain fields [21, 24]. Other reported successful techniques utilize such phenomena as acoustic emission [14, 17, 15], X-ray radiation [24, 17], and infrared thermography [24]. Recently, a method based on micro/nano-indentation of side surfaces of a cracked specimen has been tried out [30] in order to disclose the spatial (surface) distribution of mechanical properties of the tested material from which the extent of the material damage zone accumulated during the fracture process can be estimated.

In the paper an analytical method is shown which enables modelling of the FPZ during the fracture process in quasi-brittle materials, and the estimation of its size and shape. The energy dissipated within the FPZ during fracture can then be related to the extent of this zone of failure, which can result in the refining and better specification of the procedures of determination of fracture-mechanical characteristics of quasi-brittle materials, especially fracture energy [18]. In this paper, application of the method is illustrated in the context of fractures of notched beams under three-point bending and wedge-splitting test specimens.

## 2. Theoretical background

### *2.1. Classical non-linear models for quasi-brittle fracture*

As was already mentioned above, the fundamental characteristic of the tensile failure of quasi-brittle materials is the existence of the FPZ around the crack tip. This phenomenon is the reason for the non-linear fracture behaviour of these materials. Non-linear models developed for quasi-brittle fracture are divided into two basic groups according to the approach to its capture.

The simplest class of these models, which are known as equivalent elastic crack models (EECM), simulate the cohesive fracture of quasi-brittle materials by replacing the real body, which contains a crack of a certain initial length and a FPZ ahead of it, with a brittle body with an effective (sharp) crack longer than the initial one, and then forcing both bodies to exhibit the same structural behaviour. The essential advantage of these models is the linear elastic fracture mechanics (LEFM) apparatus preserved for analyses within these models. The effective crack model [16] is the representative of this group utilized in the presented technique. The effective crack length in the loaded body is determined based on the change in the secant compliance of the body between the initial and the current stage of the fracture process.

A more advanced class of models which consider the mutual cohesive effect of crack faces in the vicinity of the crack tip resulting in non-linear fracture behaviour are referred to as cohesive crack models (CCM). According to this approach a crack and the FPZ evolving around the crack tip in a quasi-brittle body is modelled by an extension $\Delta a$ of the original crack of length $a$. The crack faces are clamped by cohesive forces on a section of the cohesive crack extension from the crack tip up to a point where the crack opening displacement is critical. The progress of fracture modelled by the cohesive crack approach can be described as follows: If the external loading of the body causes such a stress distribution at the original crack tip that the stress component opening the crack exceeds the tensile strength of the material, the original crack starts to propagate and the newly formed faces of the crack extension $\Delta a$ are compressed by cohesive stress $\sigma(w)$, where $w$ is the crack opening. By this process a realistic situation is modelled in which an FPZ arises and starts to develop at the initial crack tip. When the current crack opening $w$ at the initial crack tip position exceeds a critical value $w_{\mathrm{c}}$, the whole cohesive zone starts to shift forward through the body. This situation corresponds to the separation of the FPZ from the original crack tip and the beginning of its movement through the body. An increment of the stress-free crack remains behind the FPZ. The technique for the reconstruction of FPZ size and shape described hereinafter employs tools used in the fictitious crack model

by Hillerborg et al. [8], which is a representative of cohesive crack models for quasi-brittle materials. Nowadays, the main applications of these models are their implementations into FEM codes developed for the design and assessment of concrete and reinforced concrete structures (e.g. ATENA [6], DIANA, etc.).

### 2.2. Multi-parameter fracture mechanics

Williams' solution for an elastic isotropic homogeneous 2D body with a crack [32, 13] provides an approximation of stress and deformation fields within the body by means of its expansion into a power series. For a stress tensor it holds:

$$\sigma_{ij} = \sum_{n=1}^{\infty} \left( A_n \frac{n}{2} \right) r^{\frac{n}{2}-1} f_{ij}(n,\theta) \,, \tag{1}$$

where $r$ and $\theta$ are the polar coordinates, coefficients $A_n$ are known constants and $f_{ij}$ are known functions of the angle $\theta$. A closer look at the three stress components reveals the following form:

$$\left\{ \begin{array}{c} \sigma_x \\ \sigma_y \\ \tau_{xy} \end{array} \right\} = \sum_{n=1}^{\infty} \left( A_n \frac{n}{2} \right) r^{\frac{n}{2}-1} \cdot$$

$$\left\{ \begin{array}{c} \left[2 + (-1)^n + \frac{n}{2}\right] \cos\left(\frac{n}{2}-1\right)\theta - \left(\frac{n}{2}-1\right) \cos\left(\frac{n}{2}-3\right)\theta \\ \left[2 - (-1)^n - \frac{n}{2}\right] \cos\left(\frac{n}{2}-1\right)\theta + \left(\frac{n}{2}-1\right) \cos\left(\frac{n}{2}-3\right)\theta \\ -\left[(-1)^n + \frac{n}{2}\right] \sin\left(\frac{n}{2}-1\right)\theta + \left(\frac{n}{2}-1\right) \sin\left(\frac{n}{2}-3\right)\theta \end{array} \right\} . \tag{2}$$

The first term of the series (1) or (2), respectively, is singular with regard to the distance $r$ from the crack tip (it tends to infinity for $r \to 0$) and the constant $A_1$ from this term corresponds to the stress intensity factor $K$. The second term is constant with respect to the value of $r$ and is referred to as $T$-stress. The rest of the terms take finite values for arbitrary $r$.

For an approximate description of the stress and deformation fields in the very vicinity of the crack tip (the asymptotic fields) it is possible to consider only the first term (which is the case of classical fracture mechanics) or the first two terms (the case of two-parameter fracture mechanics) of the series and ignore the terms for $n > 2$, as they converge to zero for $r \to 0$. This is possible because the failure of an ideally brittle material starts at a single point — the crack tip — for which the asymptotic description holds true.

However, in the case of a quasi-brittle material the FPZ arises and evolves around the crack tip; the size of this zone can not be neglected in relation to the dimensions of the cracked body (including the crack length). And if one needs to describe the more distant surroundings of the crack tip, higher order terms of the Williams' series must be taken into account. The FPZ size substantially exceeds a range in which the stress state can be described accurately enough only by means of classical fracture mechanics or even two-parameter fracture mechanics. Therefore, the approach when more terms of the Williams' series are used to describe stress and displacement fields in the cracked body can be referred to as an application of multi-parameter LEFM.

## 3. Estimation of the plastic zone in metallic materials

The size and shape of the plastic zone in elasto-plastic materials influences crack behaviour substantially. For an estimation of its extent two-parameter fracture mechanics (the description

of the near-crack-tip fields performed by means of $K$ and $T$ — elastic — or $J$ and $Q$ — elasto-plastic [13]) is usually utilized, as its size is relatively small (small scale yielding). In the procedure of plastic zone contour calculation an equivalent (comparative) measure of the stress field near the crack tip, determined e.g. from principal stresses with the use of the Mises or Tresca yield criterion, is compared with a particular critical value [1, 20], which is the value of yield stress or yield stress in shear, respectively. Eq. (2) can be rearranged into a closed form that for a particular angle $\theta$ explicitly returns the radius $r$. An example of the extent of plastic zones for both plane stress and plane strain conditions is depicted in fig. 1.

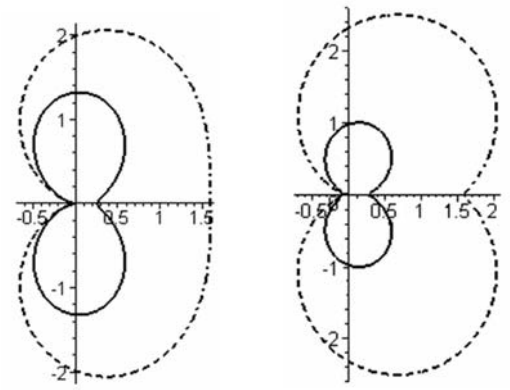


Fig. 1. Plastic zone estimation for the plane stress (dashed line) and plane strain (solid line) states for Mises (left) and Tresca (right) yield criteria (courtesy of S. Seitl [20])

## 4. Estimation of the fracture process zone in quasi-brittle cementitious materials

For the estimation of the fracture process zone in quasi-brittle materials a concept similar to that outlined in the previous section is proposed. However, essential modifications are necessary. The first concerns the size of the (plastic) zone. Cementitious materials are characterized by much lower tensile strength than metallic materials, and this results in a plastic zone[1] of much greater extent. The second reason is the cohesive manner of the quasi-brittle fracture. Cohesive stress is transferred between crack faces with an adequately small opening displacement. Therefore, the fracture process zone is much larger also in the direction opposite to the crack propagation, and this is due to the cohesive forces caused by various fracture mechanisms (taking place at the (nano-,) micro- and mezo-level).

A detailed description of the proposed method for FPZ extent estimation is performed in [27, 28]. Here we only highlight the fundamental ideas/approaches on which the technique is primarily based:

- *Equivalent elastic crack models* [16, 11] are used for the estimation of the effective crack tip during the fracture process. The effective crack model enables calculation of the effective crack length in the cracked body from the change in compliance of the body between the beginning and the current stage of the fracture process. The iterative procedure described in detail in [25] is employed.

[1]The term 'plastic' is used here because of the similarity of the concept with that described in sec. 3. In reality, the failure mechanisms in quasi-brittle cementitious composites are of a different nature (e.g. microcracking, aggregate interlock, crack bridging and branching etc. [21, 11, 24]).

- *Multi-parameter linear elastic fracture mechanics* [32, 13] is used for a description of the stress field in the specimen (not necessarily only in the very vicinity of the crack tip). Within the more distant surroundings of the crack tip, the consideration of which is essential for quasi-brittle materials with a large FPZ, higher order terms of Williams' series (eq. (2)) are taken into account.

- *The theory of plasticity* [10, 31] is employed for the determination of the zone of material where the equivalent stress exceeds the tensile strength. The Rankine failure criterion is used in this paper; however, other criteria suitable for cementitious composites, e.g. those of Drucker-Prager or Willam-Warnke [31] are possible. The contour of the Rankine equivalent stress profile is determined using the Newton's iteration method in this procedure. Direct solution of the radius $r$ and angle $\theta$ might not be appropriate if more than two terms of Williams' series are used (for up to two terms of the series the radius $r$ can be explicitly expressed as a function of the angle $\theta$).

- *Cohesive crack models* [8, 21, 5] are taken into account when introducing the cohesive law into the procedure of FPZ range estimation. This approach aids in capturing the non-linear behaviour of (cohesive) material in the FPZ. The FPZ is assembled as a union of plastic zones determined at points on the face of the propagating crack (i.e. previous crack tip positions) where the crack opening displacement is lower than its critical value.

These approaches are used within the processing of fracture test records, typically load-displacement diagrams ($P$–$d$ diagrams, see e.g. fig. 3 right), in the following sequence:

i) For individual stages of the fracture process, i.e. the points of the $P$–$d$ diagram, the length of the equivalent elastic crack is estimated by means of the effective crack model.

ii) The stress state in a body with an effective crack is approximated through Williams' power series; the number of terms in the series must be chosen with respect to the mutual relation between the assumed FPZ size/shape and the size/shape of the body (with respect to the distance between the FPZ and the free boundaries of the body).

iii) The extent of the zone where the until-now elastic material starts to fail, denoted here as $\Omega_{\mathrm{PZ}}$ (the initials 'PZ' in the subscript stands for Plastic Zone), is determined by comparing the tensile strength $f_{\mathrm{t}}$ of the material to a proper characteristics of the stress state around the crack tip (some sort of equivalent stress $\sigma_{\mathrm{eq}}$, for cementitious composites e.g. the Rankine failure criterion can be employed). As was already mentioned above, the estimation of the plastic zone boundary is performed iteratively using the Newton's method.

iv) The crack opening displacement profile for each crack tip position is calculated via appropriate LEFM formulas, e.g. from [22].

v) In agreement with the cohesive crack approach, the FPZ is supposed to extend from the zone of the current failure around the current crack tip (at stage $i$, denoted as $\Omega_{\mathrm{PZ},i}$), where the selected stress state characteristic (equivalent stress $\sigma_{\mathrm{eq}}$) exceeds the tensile strength $f_{\mathrm{t}}$, up to a point on the crack faces where the value of crack opening displacement reaches its critical value (i.e. the value of the cohesive stress drops to zero). This point corresponds to a prior stage of the fracture process (let's denote it by the subscript $k$, and the zone of failure corresponding to that stage as $\Omega_{\mathrm{PZ},k}$). For a given stage $i$ the FPZ is considered to be a union of zones $\Omega_{\mathrm{PZ}}$ with indices from the interval $\langle i, k\rangle$.

In this paper two alternative FPZ expressions are considered. In the first case, the FPZ is denoted as $\Omega_{\mathrm{FPZ,basic}}$; the union of the individual plastic zones is performed simply without any other treatment. In the second case, $\Omega_{\mathrm{FPZ,scaled}}$, the zones for the individual indices (corresponding to points on the crack face, i.e. locations of the effective crack tip during prior stages of fracture) are scaled by a factor corresponding to the relative value of the cohesive stress for those points, i.e. by $\sigma(w)/f_{\mathrm{t}}$. The envelope of $\Omega_{\mathrm{PZ}}$ zones for all stages of the fracture represents a region in which some sort of damage has taken place during the fracture process throughout the entire specimen ligament. It is denoted here as $\Omega_{\mathrm{WRAP}}$. This method of FPZ definition for the current crack tip is based on the assumption that the energy dissipation in the failure processes occurs at those points in the body where the equivalent stress $\sigma_{\mathrm{eq}}$ appropriate to prior stages of the fracture has exceeded the tensile strength $f_{\mathrm{t}}$ (failure mechanisms have started to proceed there).

The construction of an FPZ evolving during fracture in quasi-brittle materials is illustrated in fig. 2. The thick solid lines in the graph indicate the initial crack face, and the front and back boundaries of the specimen. The other lines correspond to the boundaries of the zones described above: the plastic zone $\Omega_{\mathrm{PZ},i}$ for the current crack tip position (point $i$); the plastic zone $\Omega_{\mathrm{PZ},k}$ for the last crack tip position (point $k$), where the cohesive stress is still active at the $i$-th stage of the fracture process; the fracture process zone (i.e. the union of plastic zones within the range of action of the cohesive stress) in two possible variants of its representation (basic vs. scaled); and the wrap (i.e. the union of plastic zones for all crack tip positions along the specimen ligament — the area where the material undergoes damage).

The procedure is being developed as a JAVA application under the name ReFraPro (Reconstruction of Fracture Process) [26].

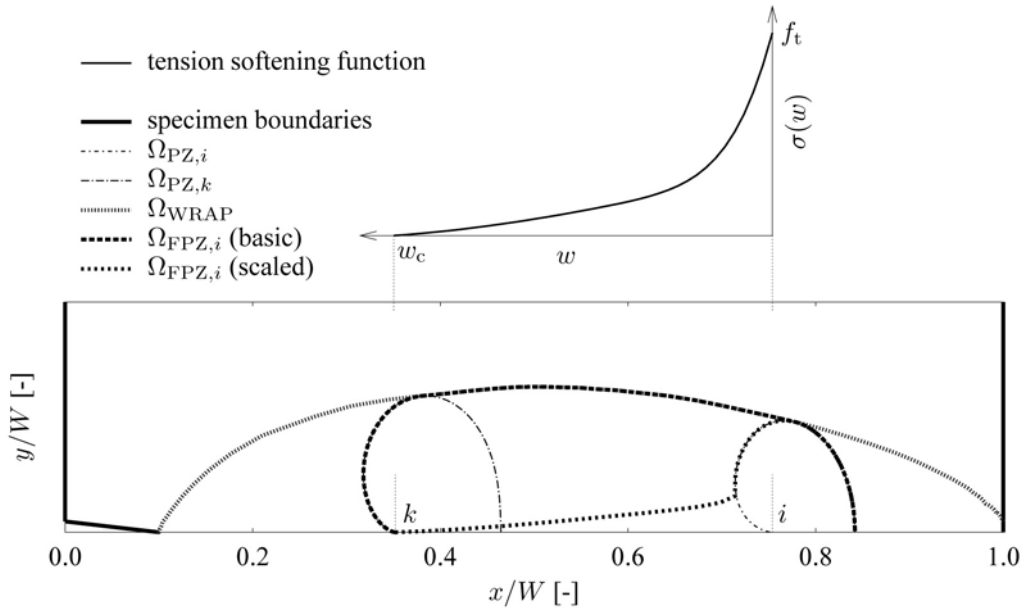


Fig. 2. FPZ construction: typical cohesive law for quasi-brittle materials (top); boundaries of the above-described formulations of zones of failure (bottom)

## 5. Examples

### 5.1. Numerically simulated test of a Single-Edge Notched beam under Three-Point Bending (SEN-TPB)

Let us consider a notched beam of dimensions $L \times W \times B$ equal to $0.48 \times 0.08 \times 0.08$ m with an initial crack/notch of length $a_0 = 0.008$ m (relative notch length $\alpha_0 = a/W = 0.1$) loaded in three-point bending (see fig. 3 left). The beam is supposed to be made of concrete with the following fracture-mechanical parameters: tensile strength $f_\mathrm{t} = 3.7$ MPa, fracture energy $G_\mathrm{F} = 93$ Jm$^{-2}$ and exhibiting exponential (Hordijk's, see e.g. [6]) softening.

The fracture test of the beam was simulated numerically using ATENA software [6] for this illustrative example. The recorded load-displacement diagram is plotted in fig. 3 right, where six stages of the fracture process are emphasized (A to F) which correspond to relative effective crack lengths $\alpha$ equal to $0.15$, $0.35$, $0.53$, $0.7$, $0.87$, and $0.97$ (respectively).

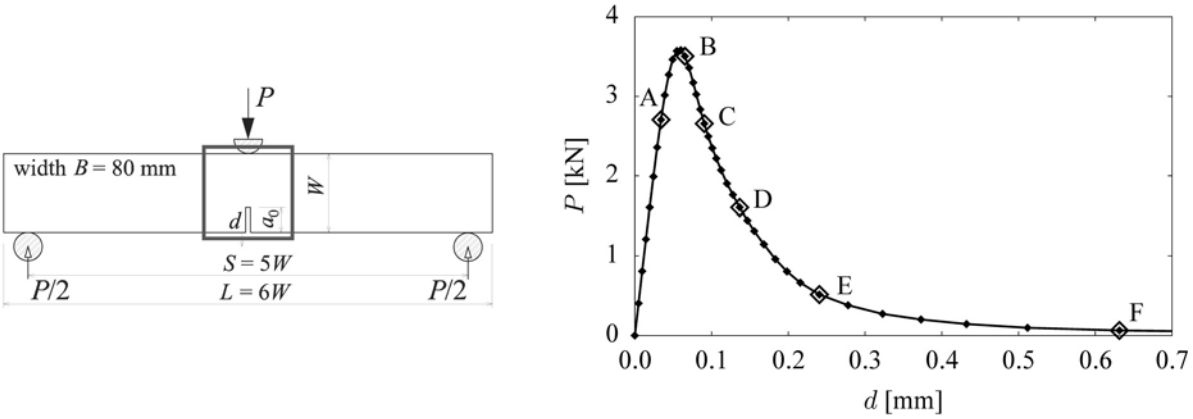


Fig. 3. SEN-TPB testing configuration (left), numerically simulated $P$–$d$ diagram for the above-described beam including values for six stages of the fracture process (right)

In fig. 4, the central part of the SEN-TPB specimen (highlighted in fig. 3 left) is displayed with a depiction of the evolution of the following quantities/phenomena corresponding to stages of the fracture process indicated in the $P$–$d$ diagram, fig. 3 right:

- Equivalent stress distribution over the specimen (left column). From this picture one can estimate the extent of the plastic zone, i.e. the zone of material damage that initiates at the current load step. The stress level corresponding to the value of tensile strength, which creates the boundary of the plastic zone, is displayed in black.

- Extent of the fracture process zone, i.e. of the area where the cohesive stress is active. Both representations of the zone considered in this paper (i.e. basic and scaled) are depicted (middle columns). The intensity of the cohesive stress is indicated by colour (gray) scale — the lightest colour indicates that the cohesive stress value is equal to tensile strength; the darkest corresponds to zero cohesive stress.

- The extent of the area where the material undergoes damage, denoted here as 'WRAP' (right column). It is created as an envelope of the plastic zones in all stages of the fracture.

For the construction of the zones four terms of the power series (see equation (2)) (the values of coefficients $A_1$ to $A_4$ for their evaluation were taken from [13]) and the Rankine

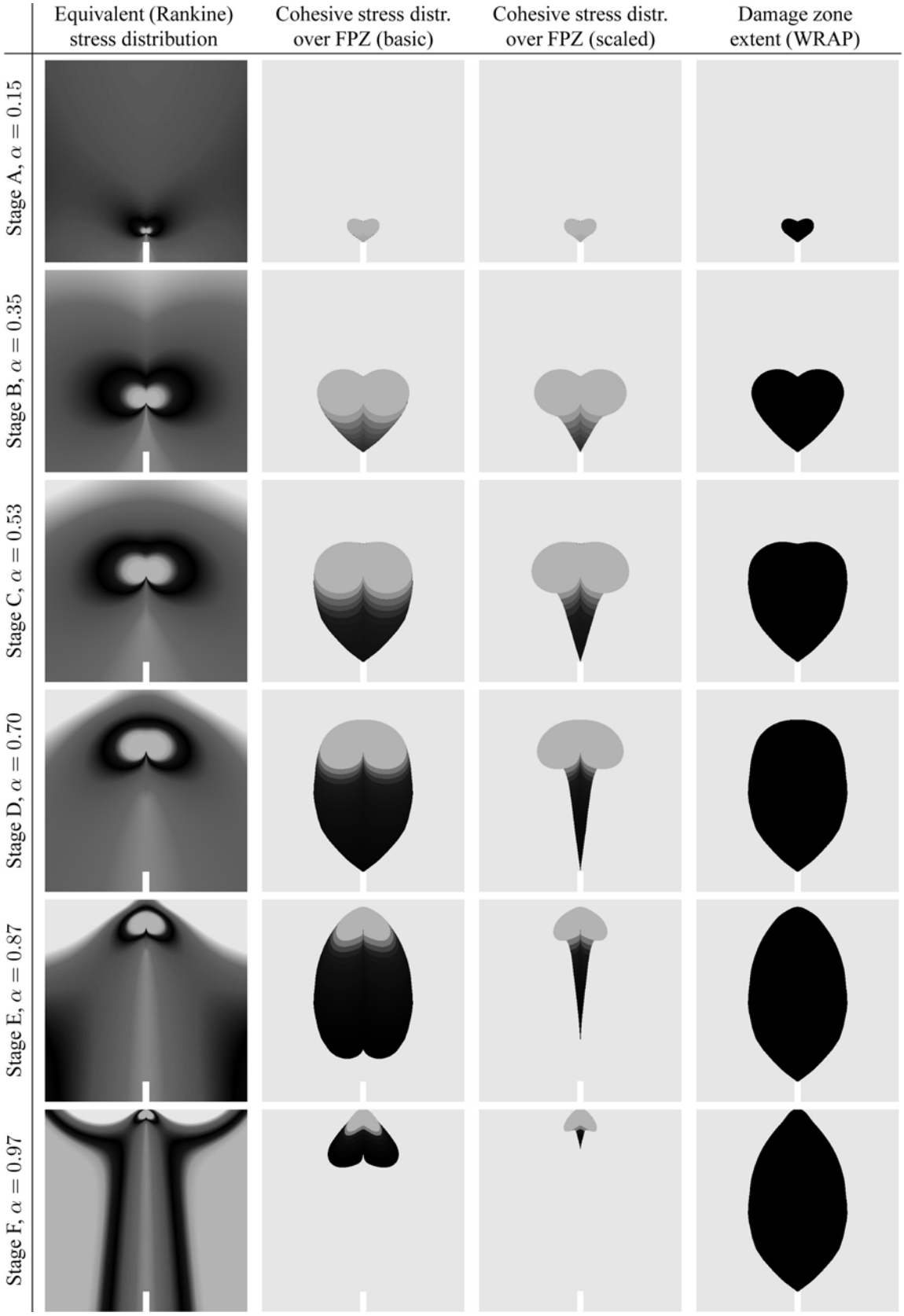


Fig. 4. Central part of the SEN-TPB specimen displaying the evolution of the equivalent (Rankine) stress distribution, the FPZ extent in both the basic and the scaled expression with indications of the intensity of the cohesive stress over the FPZ, and the WRAP extent, all for the six stages of the fracture process indicated in the load-displacement diagram in fig. 3

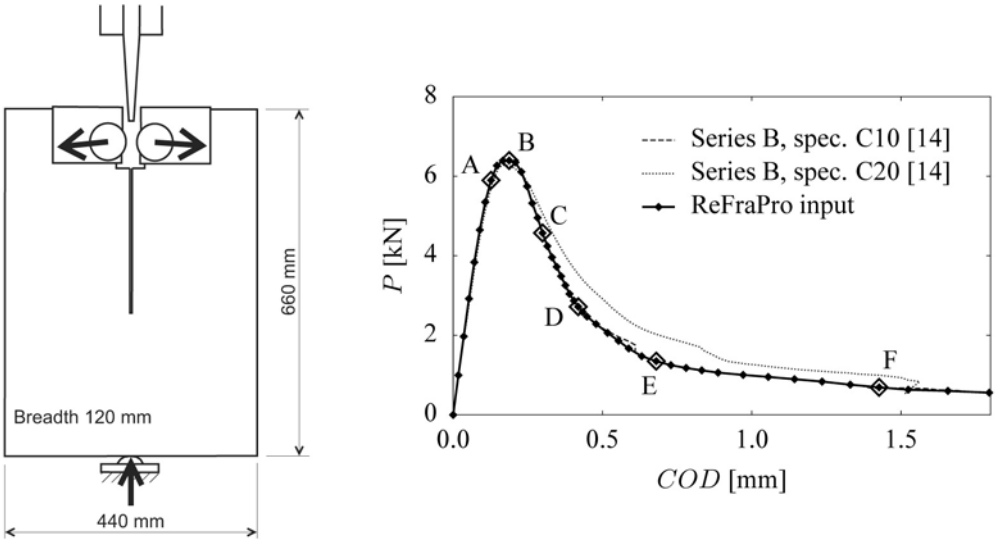


Fig. 5. Experimental set-up and dimensions of WST [14] (left) and load-displacement diagram (right)

failure criterion (in a plane stress state) are taken into account — such settings were proved to be applicable in previous studies by the authors [27, 28].

### *5.2. Experiments on Wedge-Splitting Test (WST) and SEN-TPB specimens*

Two sets of tests were selected for comparison with the results of the presented (semi-) analytical method from the rather modest amount of published works dealing with the experimental estimation of the zone of tensile failure in quasi-brittle cementitious composites. Techniques based on acoustic emission (AE) scanning were considered under the assumption that AE phenomena are similar to the approach employed within the proposed method.

The first set is the WST series conducted by Mihashi and Nomura [14]. They tested two sets of concrete and mortar specimens differing in strength and aggregate size. The experimental set-up with an indication of the specimens' dimensions is depicted in fig. 5 left. No $P$–$d$ diagrams were reported in the paper and therefore we conducted our own numerical simulations in order to estimate the structural behaviour of the specimens, which serves as an input for the developed procedure. The numerical simulation was performed in ATENA software [6]; the material model was tuned according to the compressive strength of the material reported in the paper. Two specimens were selected for which the damage zone was reported in the paper: specimens marked as C10 and C20 (both from series B, maximum aggregate size equal to 10 and 20 mm, respectively) with compressive strength $f_{\mathrm{c}} = 34.8$ and $30.5$ MPa, respectively. The simulated $P$–$d$ diagrams do not differ much, which is apparent from fig. 5, therefore a smoothed variant of the C10 $P$–$d$ curve was used as the input for the procedure. The values of the other necessary parameters were taken as being the same as for the numerical simulation: tensile strength $f_{\mathrm{t}} = 2.8$ MPa, fracture energy $G_{\mathrm{f}} = 60$ Jm$^{-2}$, and Hordijk's exponential softening curve. The other settings were analogous to those in the previous example, e.g. four terms of Williams' series (taken from [13] for CT geometry) and the Rankine failure criterion in a plane stress state.

The progress of the FPZ extent with an indication of the intensity of the cohesive stresses within it[2] for six selected stages of the fracture process (emphasized in fig. 5 right) is shown in

[2]Here another scale is applied: From light grey corresponding to $\sigma_{\mathrm{coh}} = f_{\mathrm{t}}$, through dark gray, back to light gray corresponding to $\sigma_{\mathrm{coh}} = 0$).

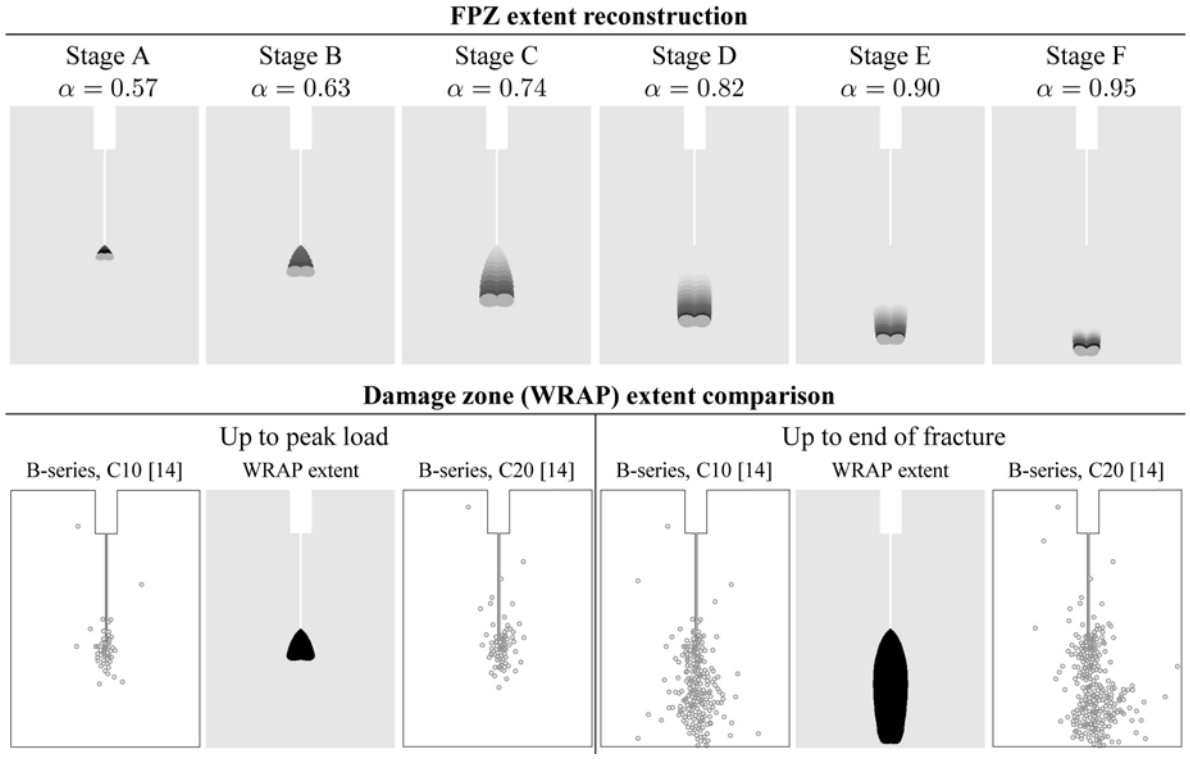


Fig. 6. WST specimen displaying the evolution of the FPZ extent (basic expression) for selected stages of the fracture process with indications of the cohesive stress intensity (top row); the WRAP extent for two stages of the fracture process in comparison to the damage zone estimated experimentally using AE [14]

the top row of fig. 6. The extent of the zones in which the AE sources were located (indicated by the small circles) in the two considered specimens by Mihashi and Nomura [14] is then compared to the WRAP extent in the bottom row of the fig. 6; for stage B (peak load) on the left, and for the end of fracture on the right. Very good agreement can be seen, especially for the final stage of the tests.

The second experimental data set was published by Muralidhara et. al [15]. They conducted SEN-TPB tests on two sizes of specimens accompanied again by AE scanning. From their series of experiments only one test (the specimen marked D2T20UB02) was reported in detail. The test configuration with the dimensions of the selected specimen is shown in fig. 7 top and the $P$–$CMOD$ curve (where $CMOD$ is the crack mouth opening displacement) present in their paper is plotted in fig. 7 left. From the reported $P$–$d$ curve (where $d$ is the mid-span deflection), see fig. 7 right, it is obvious that some problems have occurred during measurement of the deflection[3]. Therefore, numerical simulation in the ATENA software was again performed. The parameters of the material model were tuned so that the simulated and experimentally recorded $P$–$CMOD$ curves match. Using the relationship between these curves the 'true' experimental $P$–$d$ curve was subsequently reconstructed, the smoothed version of which was then used as the input for the procedure for the estimation of the damage zone extent. The values of other

[3]The displacement was probably recorded using an LVDT sensor which was fitted to the frame of the testing machine instead of using a measuring frame fitted directly to the specimen. If this is the case, the part of the displacement occuring due to the pushing of the supports into the specimen is also recorded. However, only the part of the displacement corresponding to the crack propagation is relevant for the analysis.

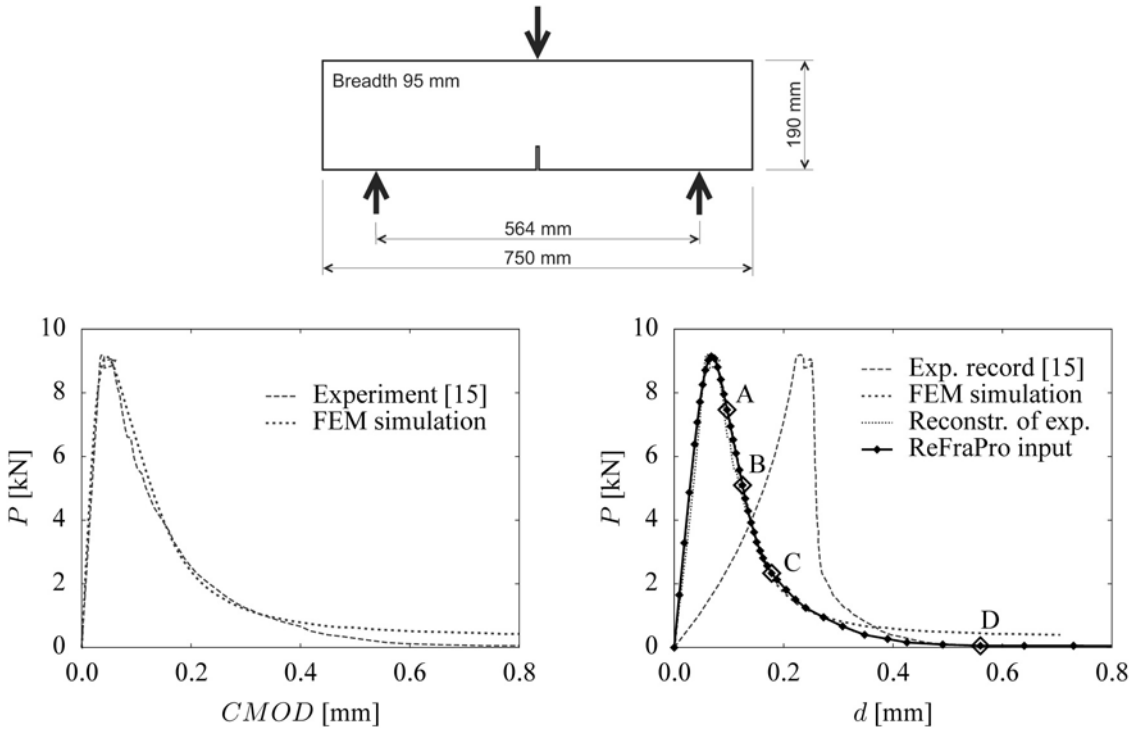


Fig. 7. Test configuration and dimensions of the SEN-TPB specimen [15] (top), load-crack mouth opening displacement diagram and load-deflection diagram, respectively (bottom)

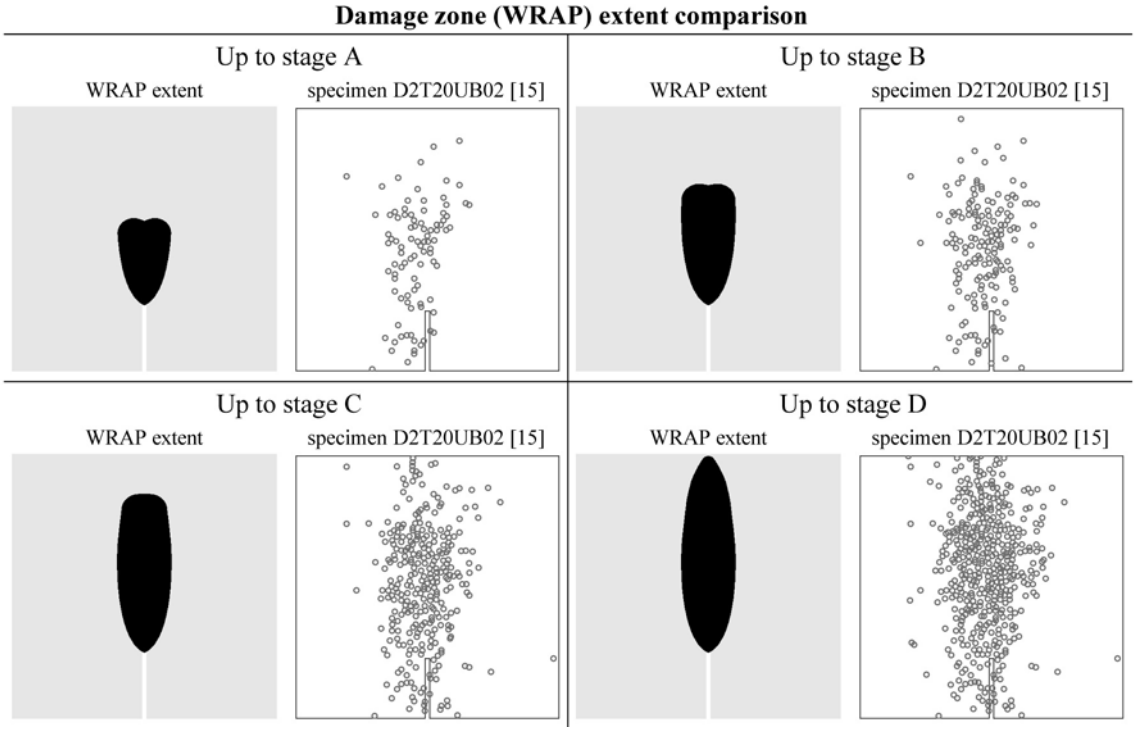


Fig. 8. Central part of the SEN-TPB specimen displaying the evolution of the WRAP extent for four selected stages of the fracture process in comparison to the experimentally estimated damage zone [15]

necessary inputs to the procedures were again equal to the values of the parameters of the material model used for the simulation: compressive strength $f_c = 42.5$ MPa, tensile strength $f_t = 4.3$ MPa, fracture energy $G_f = 90$ Jm$^{-2}$, and Hordijk's exponential softening curve. Four terms of Williams' series and the Rankine strength criterion were employed.

Fig. 8 shows a comparison between the predicted and the measured extent of the damaged zone at four stages of the test. The scatter of the AE event locations is higher whilst the density of the AE events is lower (especially for the initial stages of fracture) in the case of the Muralidhara et. al test in comparison to the Mihashi and Nomura tests. The experimentally estimated extent of the zone of cumulative damage was again predicted quite well.

## 6. Discussion of results

The first example serves as an illustration of some of the abilities of the developed procedure. The setting of the material parameter values (as the inputs to the procedure) in connection with rather small specimen dimensions results in estimation of considerable FPZ extent and WRAP width. In this case a relatively very accurate description of the stress state for the points far from the crack tip is necessary — it is obtained by using of at least 4 terms of Williams' series. In cases of larger specimens and/or more brittle materials 3 or even 2 terms may be sufficient. In contrast, for cases where the size of the FPZ takes even larger portion of the specimen's volume it is necessary to describe the stress field even more accurate.

Validation of the developed technique is performed only partially here, as the experimental data available in the literature (in most cases AE data) usually provide the zones of cumulative failure through the entire fracture process. Such zones correspond to the envelopes of the FPZs referred to as WRAPs in this paper. As can be seen in figs. 6 and 8, the agreement in this aspect is reasonable.

However, a deeper analysis of the experimental data must be made, in particular that concerning the energetic demands of the individual AE events (which can influence the extent of the damage zone, both FPZ and WRAP) and concerning the assignment of the individual AE events to the individual steps of the test (which should reveal the current extent of the FPZ). For future work it is intended to locate some experiments on such aspects in the literature and/or to conduct them ourselves. The authors also plan to compare the outputs of the procedure to data obtained by other types of experimental technique, e.g. methods based on X-ray radiation or (nano-) micro-indentation. Verifications by means of numerical tools based on lattice models are currently being investigated by the authors as a complement to the experimental evidence.

## 7. Conclusions

In the paper a method is shown which provides an estimation of the size and shape of the fracture process zone, which is a typical feature accompanying the fracture process in quasi-brittle materials. This method employs a combination of various approaches from different fields of theory of fracture mechanics and plasticity, yields reasonable results and contains considerable potential. This technique is being developed in order to create/refine procedures which enable the determination of fracture parameters of quasi-brittle materials independent of the size, shape and boundary conditions of laboratory test specimens. The procedure shall relate the energy dissipated in the FPZ to its volume and is currently under intensive investigation by the present authors.

## Acknowledgements

This outcome has been achieved with the financial support of the Ministry of Education, Youth and Sports, project No. 1M0579, within the activities of the CIDEAS research centre. In this undertaking, theoretical results gained in the project of the Czech Science Foundation, project No. GA 103/07/P403, were partially exploited.

## References

[1] Anderson, T. L., Fracture mechanics: Fundamentals and Applications, Third Edition, CRC Press, 2004.

[2] Bažant, Z. P., Analysis of work-of-fracture method for measuring fracture energy of concrete, J. Engrg. Mech. (ASCE), 122(2) (1996) 138–144.

[3] Bažant, Z. P., Kazemi, M. T., Determination of fracture energy, process zone length and brittleness number from size effect, with application to rock and concrete, Int. J. Fract. 44 (1990) 111–131.

[4] Bažant, Z. P., Oh, B. H., Crack band theory for fracture of concrete, Mater. Struct. 16 (1983) 155–177.

[5] Bažant, Z. P., Planas, J., Fracture and size effect in concrete and other quasi-brittle materials, CRC Press, Boca Raton, 1998.

[6] Červenka, V. et al., ATENA Program Documentation, Theory and User Manual, Cervenka Consulting, Prague, 2005.

[7] Duan, K., Hu, X.-Z., Wittmann, F. H., Boundary effect on concrete fracture and non-constant fracture energy distribution, Engrg. Fract. Mech. 70 (2003) 2 257–2 268.

[8] Hillerborg, A., Modéer, M., Petersson, P.-E., Analysis of crack formation and crack growth in concrete by means of fracture mechanics and finite elements, Cem. Concr. Res. 6 (1976) 773–782.

[9] Hu, X.-Z., Duan, K., Influence of fracture process zone height on fracture energy of concrete, Cem. Concr. Res. 34 (2004) 1 321–1 330.

[10] Jirásek, M., Zeman, J., Deformation and failure of materials — viscoelasticity, plasticity, fracture and damage (in Czech), Czech Technical University in Prague, 2008.

[11] Karihaloo, B. L., Fracture mechanics and structural concrete, Longman Scientific & Technical, New York, 1995.

[12] Karihaloo, B. L., Abdalla, H. M., Imjai, T., A simple method for determining the true specific fracture energy of concrete, Mag. Concr. Res. 55 (2003) 471–481.

[13] Knésl, Z., Bednář, K., Two-parameter fracture mechanics: Calculation of parameters and their values (in Czech), Institute of Physics of Materials, Czech Academy of Sciences, 1998, Brno.

[14] Mihashi, H., Nomura, N., Correlation between characteristics of fracture process zone and tension-softening properties of concrete, Nuclear Engineering and Design 165 (1996) 359–376.

[15] Muralidhara, S., Raghu Prasad, B. K., Eskadri, H., Karihaloo, B. L., Fracture process zone size and true fracture energy of concrete using acoustic emission, Construction and Building Materials 24 (2010) 479–486.

[16] Nallathambi, P., Karihaloo, B. L., Determination of specimen-size independent fracture toughness of plain concrete, Mag. Concr. Res. 38 (1986) 67–76.

[17] Otsuka, K., Date, H., Fracture process zone in concrete tension specimen. Engrg. Fract. Mech. 65 (2000) 111–131.

[18] RILEM Committee FMT 50, Determination of the fracture energy of mortar and concrete by means of three-point bend test on notched beams, Mater. Struct. 18 (1985) 285–290.

[19] Řoutil, L., Veselý, V., Keršner, Z., Seitl, S., Knésl, Z., Fracture process zone size and energy dissipated during crack propagation in quasi-brittle materials, Proceedings of 17th European Congress on Fracture – ECF 2008 (book of abstracts + CD-ROM), J. Pokluda, P. Lukáš, P. Šandera, I. Dlouhý (eds.), Vutium, Brno, 2008, 97 + CD 8 p.

[20] Seitl, S., A study of the plastic zone within the framework of two-parameter fracture mechanics (in Czech), Proceedings of Computational Mechanics 2002, Nečtiny, 2002, 423–430.

[21] Shah, S. P., Swartz, S. E., Ouyang, C., Fracture mechanics of structural concrete: applications of fracture mechanics to concrete, rock, and other quasi-brittle materials, John Wiley & Sons, Inc., New York, 1995.

[22] Tada, H., Paris, P. C., Irwin, G. R., The stress analysis of cracks handbook, 3rd ed., Professional Engineering Publishing, Ltd., Bury St. Edmunds, UK, 2000.

[23] Trunk, B., Wittmann, F. H., Influence of size on fracture energy of concrete, Mater. Struct., 34 (2001) 260–265.

[24] van Mier, J. G. M., Fracture Processes of Concrete: Assessment of Material Parameters for Fracture Models, CRC Press, Inc., Boca Raton, 2007.

[25] Veselý, V., Parameters of concrete for description of fracture behaviour. PhD Thesis, Brno University of Technology, Faculty of Civil Engineering, Brno, 2004 (in Czech).

[26] Veselý, V., Frantík, P., *ReFraPro — Reconstruction of Fracture Process*, Java application, 2008.

[27] Veselý, V., Frantík, P., Development of fracture process zone in quasi-brittle bodies during failure, Proceedings of Engineering Mechanics 2009, J. Náprstek a C. Fischer (eds.), Svratka, Czech Rep., Institute of Theoretical and Applied Mechanics, v.v.i., Academy of Sciences of the Czech Republic, 288–289 + 1 393–1 404 (CD – in Czech).

[28] Veselý, V., Frantík, P., Keršner, Z., Cracked volume specified work of fracture, Proceedings of the 12th Int. Conf. on Civil, Structural and Environmental Engineering Computing, B. H. V. Topping, L. F. Costa Neves and R. C. Barros (eds.), Funchal, Civil-Comp Press, 2009.

[29] Veselý, V., Řoutil, L., Keršner, Z., Structural geometry, fracture process zone and fracture energy, Proceedings of Fracture Mechanics of Concrete and Concrete Structures (Proc. FraMCoS-6), Al. Carpinteri, P. Gambarova, G. Ferro, G. Plizzari (eds.), Catania, Italy, Taylor & Francis/Balkema, vol. 1 (2007) 111–118.

[30] Veselý, V., Keršner, Z., Němeček, J., Frantík, P., Řoutil, L., Kucharczyková, B., Estimation of fracture process zone extent in cementitious composites, Chem. Listy 104 (2010) 382–385.

[31] Wikipedia, the free encyclopedia — Stress (mechanics), Yield surface, http://en.wikipedia.org.

[32] Williams, M. L., On the stress distribution at the base of a stationary crack, ASME J. Appl. Mech. 24 (1957) 109–114.